Uncertainty relation and quantum Cheshire-Cat: studied with neutron polarimeter and interferometer

Yuji Hasegawa

Atominstitut, Technische Universität Wien (TU-Wien), A-1020 Wien, Austria

Fundamental phenomena in quantum mechanics are investigated by the use of matter-wave optics: in the studies neutron polarimeter and interferometer are exploited. Successive measurements of 1/2-spin of the neutron are carried out to test the error–disturbance uncertainty relation. The experimental results confirm the violation of Heisenberg's original reciprocal relation for measurement error and disturbance, and the validity of the reformulated generally valid relation. In addition, as an example of a counterfactual phenomenon of quantum mechanics, interferometric experiment is performed to observe the so-called quantum Cheshire-Cat: a particle and its magnetic moment travel through the interferometer along different beam paths. The results of our experiment suggest that, with suitable pre- and post-selections, neutrons travel along one of the arms of the interferometer, while their spin is located in the other arm.

Keywords: Cheshire-Cat, interferometer, polarimeter, neutron, uncertainty relation.

Introduction

SINCE the early stages of the development of quantum theory, peculiarities predicted by the theory have fascinated and even confused everyone, not only the interested public but also physicists. One of the most astonishing phenomenon displayed by quantum systems at the atomic scales (or even larger) is the wave–particle duality, which compels us to perceive quanta, such as electrons, neutrons and photons, as entities behaving simultaneously both like waves as well as particles[1]. The double-slit experiment, in particular with single particles, has been serving as the best example to view the central mystery in quantum mechanics[2]. Wave and particle properties, both familiar to us in classical physics, emerge and, moreover, it displays intrinsically probabilistic nature of quantum-mechanical predictions. In the quantum version of the double-slit experiment, when both slits are open and particles like neutrons, electrons, molecules and so forth are sent, there appear 'interference fringes' in the final distribution at the screen. It sounds reasonable if one accepts the situation where particles, which cannot be divided into pieces, hit both slits simultaneously and 'an effect' from both opening with wave-like property reaches the screen, exhibiting fringe pattern due to constructive and destructive interference effects. It is worth noting here that non-local effects, not in a sense of quantum *kinematics* observed in two-particle correlation but in a sense of quantum *dynamics* described by quantum equation of motion[3], are clearly observed in the quantum version of the double-slit experiment.

Optical experiments with massive particles such as neutrons, electrons, atoms and molecules play a significant role while testing peculiar phenomena predicted by quantum theory. Note that such an important physical concern is sometimes easily forgotten but lies beneath that the (non-relativistic) Schrödinger equation can be directly applied in describing the time-evolution of quantum state of massive quantum system: de Broglie waves with a wavelength $\lambda = h/mv$, spin quantum numbers s, canonical commutation relation such as $[x_i, p_j] = i\hbar\delta_{ij}$, etc. are purely quantum-mechanical features and cannot be found in classical mechanics. The perfect crystal neutron interferometer was invented in 1974 at the Atominsitut, Vienna[4], which opened up a new era of the fundamental studies of quantum mechanics with matter-waves. By taking advantage of the macroscopic beam separation of several centimetres, the wave-like aspect of neutrons is observed explicitly and exploited for the fundamental investigations of quantum mechanics[5,6]. Another neutron optical approach is spin interferometry. A principle that is utilized in neutron polarimetry[7,8] is that spin eigenstates are manipulated with a high degree of accuracy and the interference between these eigenstates or their entangled degrees of freedom is observed, mostly without spatial beam separation. Due to its superior resilience against environmental perturbations, it complements split-beam experiments. The advantages of this approach are: (1) the instrument is robust: rather insensitive to environmental disturbances, and (2) highly efficient (>99%) manipulations are possible: final contrast reaching about 99%.

From the very beginning, neutron interferometer experiments have been established as one of the most powerful tools for investigations of quantum-mechanical

e-mail: hasegawa@ati.ac.at

phenomena on a fundamental basis. Over the past decades, neutron interferometry has provided excellent opportunities for many types of interferometer experiments with neutrons, ranging from fundamental quantum investigations to application measurements, such as precise measurements of coherent neutron scattering lengths. The former exploits the neutron interferometry as a matter-wave interference experiment and the latter is frequently required for other types of neutron scattering spectroscopy. Consequences of the nonrelativistic Schrödinger equation for matter-waves can be studied, for instance, with electrons, atoms, ions and molecules. Features of neutron interferometry, such as macroscopic-scale experiments, high detector efficiency, low decoherence rate, and high-efficiency manipulation rate, make it a unique strategy for quantum-mechanical investigations. Recently, neutron polarimeter experiments have begun to serve as another tool to verify the basic concepts of quantum mechanics. There, basis used in the experiment is spanned not by two paths $|\mathrm{I}\rangle$ and $|\mathrm{II}\rangle$, but by spin eigenstate $|\uparrow\rangle$ and $|\downarrow\rangle$. With this device, for instance, the non-commutation of the Pauli spin operator[9] and a number of geometric phase measurements[10] are carried out. The implicit polarization interference scheme allows us to perform textbook-like demonstrations of quantum mechanics with high efficiency and stability.

In this article, recent experiments with the neutron interferometer and the polarimeter are presented. The first experimental test of the reformulated error–disturbance uncertainty relation is tested: successive measurements of neutron's spin[11,12] exhibit the violation of the naive error–disturbance relation by Heisenberg and confirm the validity of a new universally valid error–disturbance relation by Ozawa[13,14]. In addition, a paradoxical phenomenon within the framework of quantum mechanics has been found recently[15,16] and named after the 'Cheshire-Cat' featured in Lewis Carroll's novel *Alice in Wonderland*: she disappears, leaving her grin behind. The quantum Cheshire-Cat emerges, if a quantum system is subjected to certain pre- and post-selections. It can behave as if a particle itself and its property are spatially separated. In our neutron interferometer experiments, we have successfully observed the quantum Cheshire-Cat[17]. The neutron system behaves as if neutrons travel along one beam-path of the interferometer, while their magnetic moment (neutrons are spin-1/2 fermions) travels along the other.

Error–disturbance uncertainty relation

The uncertainty principle refers to intrinsic indeterminacy of quantum mechanics and ranks among the most famous statements of modern physics[18]. It was Heisenberg[19] who first formulated the uncertainty relation as a limitation of accuracies of position and momentum measurements. Later on, the uncertainty relation was reformulated in terms of standard deviations, which denote only the statistical quantity and neglect neither the disturbance due to interactions in a quantum measurement nor measurement error[20,21]. It was know that the validity of Heisenberg's original relation is justified only under limited circumstances, and Ozawa[13,14] proposed a new universally valid error–disturbance uncertainty relation. Here, we describe a successive spin measurement of neutrons that allows determining the error of a spin-component measurement and the disturbance caused on another spin-component measurement[11]. The results confirm that both error and disturbance completely obey Ozawa's relation, but often violate the Heisenberg's relation.

From Heisenberg to universally valid uncertainty relation

In 1927, Heisenberg[19] proposed the uncertainty relation for the error $\varepsilon(Q)$ of a electron's position measurement and the disturbance $\eta(P)$ of the momentum measurement in a form $\varepsilon(Q)\eta(P) \sim \hbar/2$, where $\hbar$ is Planck's constant divided by 2π (here, we use $\hbar/2$ for consistency with modern treatments). The reciprocal relation $\sigma(Q)\sigma(P) \geq \hbar/2$ for standard deviations $\sigma(Q)$, $\sigma(P)$ of position and momentum was proved by Kennnard[20], which was generalized to arbitrary pairs of observables A, B by Robertson[21] as $\sigma(A)\sigma(B) \geq 1/2|\langle\psi|[A, B]|\psi\rangle|$, in any state. Here, $[A, B]$ represents the commutator $[A, B] = AB - BA$, and the standard deviation is defined as $\sigma(A)^2 = \langle\psi|A^2|\psi\rangle - \langle\psi|A|\psi\rangle^2$. Robertson's[21] relation with standard deviations has a mathematical basis. Nevertheless, the proof of the reciprocal relation for the error, a generalized form of Heisenberg's error–disturbance uncertainty relation

$$\varepsilon(A)\eta(B) \geq \frac{1}{2}|\langle\psi|[A, B]|\psi\rangle|, \tag{1}$$

is not straightforward. Recently, rigorous and general theoretical treatments of quantum measurements have revealed the failure of Heisenberg's relation, i.e. eq. (1), and derived a new universally valid uncertainty relation[13,14] given by

$$\varepsilon(A)\eta(B) + \varepsilon(A)\sigma(B) + \sigma(A)\eta(B) \geq \frac{1}{2}|\langle\psi|[A, B]|\psi\rangle|. \tag{2}$$

Here, the error $\varepsilon(A)$ is defined as the root mean square (rms) of the difference between the output operator O_A actually measured and the observable A to be measured, whereas the disturbance $\eta(B)$ is defined as the rms of the change in the observable B during the measurement. Note that the additional second and third terms imply a new accuracy limitation, which does not necessarily follow the trade-off relation of error and disturbance.

Uncertainty relation in successive spin measurements

Here, the validities of two forms of error–disturbance relations, eqs (1) and (2) are experimentally tested with successive spin measurements of the neutron. The experimental set-up is depicted in Figure 1. Observables A and B are set as σ_x and $\sigma_{\phi B}$ (an observable lying on the equator with the azimuthal angle ϕ_B of the Bloch sphere). The initial state $|\Psi\rangle$ is set to be $+z$ spin state, $|+z\rangle$. In order to observe dependence of the error $\varepsilon(A)$ and the disturbance $\eta(B)$ on the output observable, $O_A = \sigma_x \cos\phi_{OA} + \sigma_y \sin\phi_{OA}$ (instead of exactly measuring $A = \sigma_x$), the apparatus M1 is designed to actually carry out measurements of adjustable observables. For determination of the error $\varepsilon(A)$ and the disturbance $\eta(B)$, the method proposed by Ozawa[14] is used.

The experiment was carried out at the research reactor facility TRIGA Mark II of TU-Vienna. The monochromatic neutron beam is polarized crossing a super-mirror polarizer and two other super-mirrors are used as analysers. The guide field together with four DC spin rotator coils, induces Larmor precession to allow state preparation and projective measurements of O_A in M1 and B in M2. To test the error–disturbance uncertainty relation in eqs (1) and (2), the standard deviations $\sigma(A)$, $\sigma(B)$, the error $\varepsilon(A)$ and the disturbance $\eta(B)$ are determined from the experimentally obtained data: the measurements of the standard deviations $\sigma(A)$ and $\sigma(B)$ are carried out by M1 and M2 separately, whereas error $\varepsilon(A)$ and disturbance $\eta(B)$ are determined by successive projective measurements utilizing M1 and M2.

Results of the measurements are shown in two cases: (i) $B = \sigma_y$ and (ii) $B = \sigma_x \cos(5\pi/6) + \sigma_y \sin(5\pi/6)$. The azimuthal angle of ϕ_{OA} of the output observable O_A is varied from 0 to 2π. From the obtained values of error $\varepsilon(A)$, disturbance $\eta(B)$, standard deviations $\sigma(A)$ and $\sigma(B)$, the Heisenberg error–disturbance product $\varepsilon(A)\eta(B)$ and the universally valid expression $\varepsilon(A)\eta(B) + \varepsilon(A)\sigma(B) + \sigma(A)\eta(B)$ are plotted as a function of the detuned azimuthal angle ϕ_{OA} in Figure 2. The figures illustrate the fact that the universally valid expression is always larger than the limit, whereas the Heisenberg product is often below the limit. In particular, in the range $\phi_{OA} = [0, \pi/2]$ of Figure 2 *a*, a trade-off relation between the error and the disturbance is observed, and the Heisenberg product is always below the limit, which is reported in more detail in the literature[11,12]. In Figure 2 *b*, the situation is observed where the universal expression actually touches the limit, which corresponds to the case where the equal sign of the inequality eq. (2) really occurs.

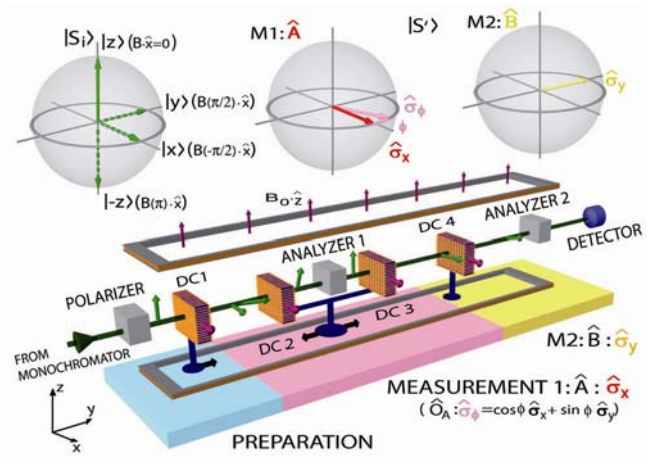

Figure 1. Set-up of the neutron optical test of error–disturbance uncertainty relation.

Ex-post uncertainty relations

The neutron's spin measurement of ours is the first experimental test of the error–disturbance uncertainty relation. The validity of the new relation (eq. (2)) proposed as a universally valid error–disturbance relation is demonstrated; moreover, the failure of the old relation as a reciprocal relation between the error and disturbance is also illustrated. This experiment stimulated further

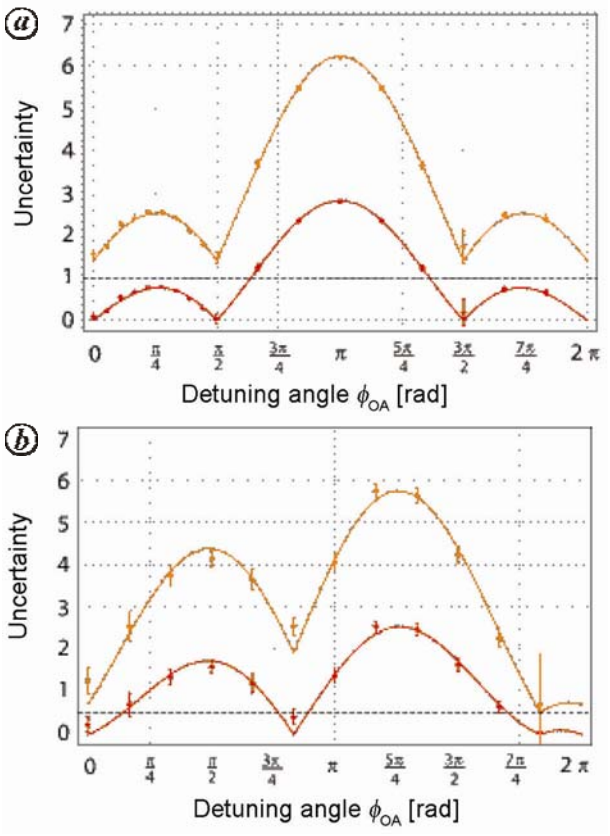

Figure 2. Experimentally determined values of the universally valid uncertainty relation: (i) $\varepsilon(A)\eta(B) + \varepsilon(A)\sigma(B) + \sigma(A)\eta(B)$ (orange), and (ii) $\varepsilon(A)\eta(B)$ (red) are plotted as a function of the detuning angle ϕ for the cases (***a***) $B = \sigma_y$ and (***b***) $B = \sigma_x \cos(5\pi/6) + \sigma_y \sin(5\pi/6)$.

studies on the error–disturbance uncertainty relation: in fact, experiments using a photonic system were conducted[22–24]. All measurements concern polarization of the photon, which is described as a two-level quantum system in the same manner as the 1/2-spin of neutrons. Afterwards, a significant extension in theory was made; a tighter relation was obtained[25] and its validity was confirmed by experiments[26,27]. Now, uncertainty relations have again become a hot topic in quantum physics, more than 80 years after the publication of the first account of the uncertainty principle by Heisenberg.

In writing the paper, we are actually aware of the fact that '*our result demonstrates that the new relation solves a long-standing problem of describing the relation between measurement accuracy and disturbance, and sheds light on fundamental limitations of quantum measurements, for instance on the debate of the standard quantum limit for monitoring free-mass position*'[11]. Nevertheless, ex post facto critical analysis was made[28]: for instance, state dependence of the error and the disturbance by Ozawa are claimed, and state-independent definitions of error and disturbance are proposed to reconstruct the error–disturbance uncertainty relation in the same form as the original one proposed by Heisenberg[29]. The newly defined error and disturbance are 'state independent, each giving the worst-case estimates across all states': this allows overestimate of the measurement error and disturbance. This claim is immediately criticized by two papers of some authors of the experimental papers[30,31]: physical analysis in the former figures out the new definition as 'disturbance power', and mathematical consideration in the latter reveals breakdowns of the new definition.

Furthermore, a paper has been published which deals with 'operational constraints' on the measures of the error and disturbance[32]: it is stated that, since '*only the change in the measurement statistics can be detected by the measurement*', '*a measurement cannot be treated as disturbed if its outcome statistics is identical to the one for the perfect measurement*' (underlines given by the author). The fact that this view does not accomplish its intended purpose is clearly seen in the first experimental test of ours: as we already emphasized as '*It is worth noting that the mean value of the observable A is correctly reproduced for any detuning angle ϕ, that is, $\langle +z|O_A| + z\rangle = \langle +z|A| + z\rangle$, so that the projective measurement of O_A reproduces the correct probability distribution of A, whereas we can detect the non-zero r.m.s. error $\varepsilon(A)$ for $\phi \neq 0$.*'[11] It is physically reasonable that the difference of the observable $O_A \neq A$ for $\phi \neq 0$, which is realized in the experiment, leads to the *error* of the measurement, even though the measurement results are identical. This is unsurprisingly understood when one considers, for instance, an apparatus which (is broken and) always gives the results of the measurement as (+1) and (–1) with a fifty–fifty chance: can one regard this not a causal but an accidental coincidence as (physically) error-free? As far as *physical* consequences are concerned, causal differences, which can appear even in an operational form, are resources of the measurement error/disturbance; modern quantum measurement schemes, i.e. process tomography or that in combination with weak values, can actually reveal the operational difference. The *functional* differences, emerging only in the final results, can be considered as *informational* aspects of the measurements. Indeed, another form of noise–disturbance uncertainty relation in context of *information-theoretic approach* has been derived[33,34], where the correlations of the measurement results are considered as the resource.

Quantum Cheshire-Cat: paradoxical phenomenon in quantum mechanics

From its very beginning, quantum theory has revealed extraordinary and counterintuitive phenomena, such as Schrödinger's Cat[35] and quantum nonlocality[36]. Quantum mechanics is still capable of exhibiting counterfactual phenomena. For instance, Hardy paradox describes a contradiction between the classical picture and the outcome of quantum mechanics[37]: joint weak measurements of trajectories of a photon pair on a post-selected state in a pair of Mach–Zehnder interferometers reveal a negative value for a joint probability of locations[38,39]. Here, a weak measurement is a technique proposed by Aharonov, Albert and Vaidman (AAV)[40]: a weak value is defined as $\hat{A}_w = \langle \Psi_{\text{fin}}|\hat{A}|\Psi_{\text{ini}}\rangle / \langle \Psi_{\text{fin}}|\Psi_{\text{ini}}\rangle$ with certain pre- and post-selected systems, represented by $|\Psi_{\text{ini}}\rangle$ and $|\Psi_{\text{fin}}\rangle$ Weak values can be obtained by so-called weak measurements with minimal disturbance on the measured system, contrary to conventional projective measurements. Note that weak values lie over the range of eigenvalues[41,42], and may even be complex[43]. The weak value was also used as an amplifier to discover new physical effects that could not be otherwise detected[44]. Recently, another counterfactual paradox, called quantum Cheshire-Cat, attracted attention: in pre- and post-selected circumstances, a cat, i.e. a particle, is found in one place and its grin, e.g. a spin in another[15,16].

Quantum Cheshire-Cat in a neutron interferometer experiment

Recently, a paradoxical phenomenon within the framework of quantum mechanics has been found and named after the 'Cheshire-Cat' featured in Lewis Carroll's novel *Alice in Wonderland*: she disappears, leaving her grin behind. The key issues are proper pre- and post-selections: a particle is prepared in a certain initial state, afterwards affected by appropriate post-selection. The quantum Cheshire-Cat emerges: it can behave as if a particle and its property are spatially separated[15,16]. We accomplished the first observation of the quantum

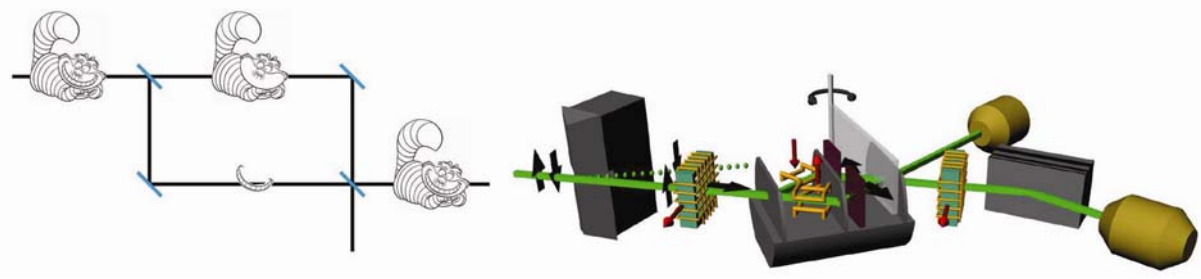

Figure 3. (Left) The concept of quantum Cheshire-Cat. (Right) Experimental set-up with neutron interferometer. In the Mach–Zehnder interferometer, a Cat is in the upper beam path while the grin is in the lower beam path. In the neutron interferometric version, an incident beam is polarized and falls on the interferometer. The pre-selected state $|\Psi_i\rangle$ is generated in the interferometer and post-selection on the state $|\Psi_f\rangle$ is carried out on the beam leaving the interferometer.

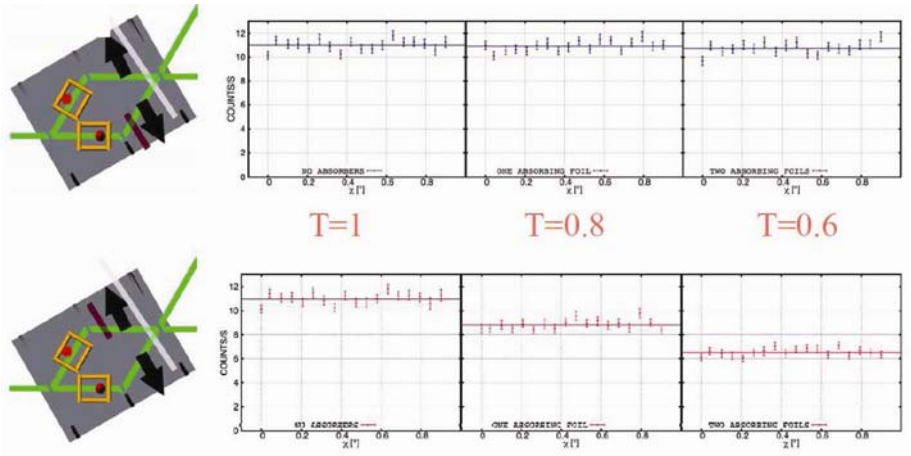

Figure 4. Weak measurements of the population of the neutron in the beam path in the interferometer. Absorbers with transmissivity of 1, 0.8 and 0.6 are inserted in one of the beam paths in the interferometer. In the upper panel, absorbers in path I (lower path) have no effect on the intensity. In the lower panel, the intensity of path II (upper path) decreases by inserting absorbers. Now, one finds neutrons in path I.

Cheshire-Cat in a neutron interferometer. In our neutron interferometer experiment, the neutron plays a role of the cat and its spin does the grin[17]. The concept of quantum Cheshire-Cat as well as the experimental set-up are depicted in Figure 3. The pre- and post-selected states are set as

$$\begin{cases} |\Psi_i\rangle = \dfrac{1}{\sqrt{2}}\{|+x\rangle|I\rangle + |-x\rangle|II\rangle\}, \\ |\Psi_f\rangle = \dfrac{1}{\sqrt{2}}|-x\rangle\ \{|I\rangle + |II\rangle\}. \end{cases} \tag{3}$$

To characterize the population of the neutron in the interferometer and the location of its spin, weak values of the observables, $\hat{\Pi}_j \equiv |j\rangle\langle j|$ and $\langle\hat{\sigma}_z^s\hat{\Pi}_j\rangle$ with $j = I$ and II are determined. Theory predicts the values, $\langle\hat{\Pi}_{\mathrm{I}}\rangle_{\mathrm{w}} = 0$, $\langle\hat{\Pi}_{\mathrm{II}}\rangle_{\mathrm{w}} = 1$, $\langle\hat{\sigma}_z^s\hat{\Pi}_{\mathrm{I}}\rangle_{\mathrm{w}} = 1$, and $\langle\hat{\sigma}_z^s\hat{\Pi}_{\mathrm{II}}\rangle_{\mathrm{w}} = 0$.

In the experiment, the incident neutron beam is polarized using magnetic prisms and the initial state $|\Psi_i\rangle$ is generated. A pair of water-cooled spin-rotators are employed in the interferometer. After the relative phase χ between the two beams is adjusted by the phase shifter and the beams are recombined at the last plate of the interferometer, the O-beam (interfering beam leaving the interferometer in the forward direction) is affected by spin analysis: the postselection is carried out by a combination of the phase shifter and the spin analysis system. Weak measurements of population of the neutron and the location of its spin are performed by the use of absorbers and additional spin rotation in one of the beams in the interferometer.

Here, we explain the experimental results qualitatively. First, in the measurements of population of the neutron, an absorber is inserted in one of the beam paths in the interferometer. Typical results are shown in Figure 4: the absorbers in the beam path I (lower path) do not affect the final intensity of the O-beam with a spin analysis, while intensity of path II (upper path) decreases according to the strength of the absorber. This suggests that the neutrons are travelling through the interferometer, following beam path I. Next, in the measurement of location of the spin of neutron, a fairly weak magnetic field is applied in one of the beam paths in the interferometer.

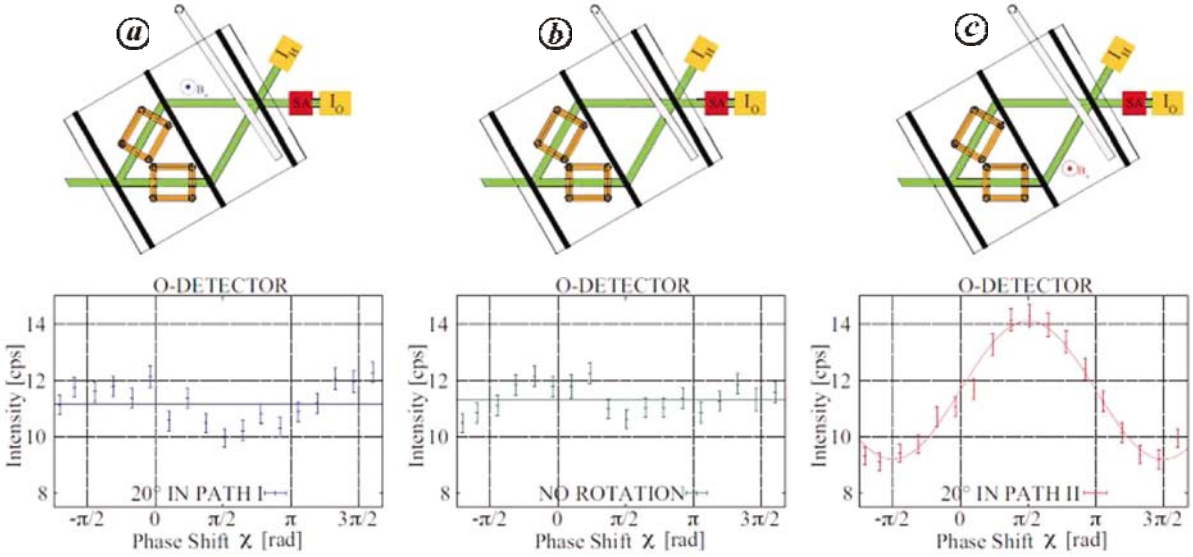

Figure 5. Weak measurements of the location of spin of the neutrons in the interferometer. A weak magnetic field is applied in one of the beam paths of the interferometer. ***b***, Interferogram without a magnitic field plotted as a reference. ***a***, A magnetic field in path II (upper path) has (practically) no effect on the interferogram. ***b***, A clear interferogram appears by applying a magnetic field in path I (lower path). Now, one finds neutron's spin in path II.

Typical results are shown in Figure 5: the magnetic field in the beam path II (upper path) does not affect the final intensity of the O-beam with a spin analysis, whereas sinusoidal intensity modulation appears by applying the magnetic field in path I (lower path). This suggests that the spin of the neutron, in turn, is travelling through the interferometer, following beam path II. These results are consistent with the theoretical prediction[16]: neutrons, which are affected by appropriate pre- and post-selection, behave as if they travel in one of the paths, whereas their spin is disembodied and located in the other path.

Quantum Cheshire-Cat in quantum mechanical evolution

A question may arise whether one can view the quantum Cheshire-Cat alternatively by following the evolution of the wave function of the neutron. This argument is clarified here. Looking at the experimental set-up depicted in Figure 3, the population of the neutrons can be intuitively understood. The spin analysis behind the interferometer allows only neutrons with spin in the forward direction to transmit. These are exactly the neutrons in the upper beam path: the neutrons in the lower beam path will be filtered out by the spin analyser. The first measurement shows exactly this situation (Figure 4). How about the location of the spin of the neutron? In the measurement of spin, a weak magnetic field is applied: the spin vector in each beam path is rotated. That is, the spin in the forward/backward direction is deviated from the original direction by the angle α, followed by spin analysis in forward direction. Since the spin analysis is described by the projection, the intensities after the spin analysis on spins deviated from the parallel and the anti-parallel are proportional to $\cos(\alpha/2)$ and $\sin(\alpha/2)$ respectively. Therefore, the differences in intensity with and without the weak magnetic field result in $\cos(\alpha/2) - 1 \approx -\alpha^2/8$ (parallel spin in the upper path) and $\sin(\alpha/2) - 0 \approx \alpha/2$ (anti-parallel spin in the lower path). This means, the influence of the magnetic field in the upper path is in the first order of α, while that in the lower path is in the second order. For the parameter $\alpha \sim 15°$ realized in the experiment, the former becomes 0.13, while the latter is 0.0085: the former is more than one magnitude larger the latter. This phenomenon is clearly observed in the interferograms obtained in the second measurement (Figure 5). A major change in the case of the magnetic field in the lower path for small α is attributed to the spin travelling through the lower path.

Concluding remarks

The test of the error–disturbance uncertainty relation presented here is actually the first experimental test of this kind. The demonstration of ours is the first experimental evidence for the invalidity of the old (by Heisenberg) and validity of the new (by Ozawa) uncertainty relation. It should be emphasized here that this experiment opens up a new era of uncertainty relation where, more than 80 years after the Heisenberg's original publication, the topic is taken up again for hot discussions both from the theoretical and experimental point of view. Our result clarifies a long standing problem of describing the relation between measurement accuracy and disturbance, and

sheds light on fundamental limitations of quantum measurements. It is fair to say that our experiment activates this research field. One cannot emphasize too much the importance of amending such a fundamental concept not only from a purely academic but also a practical point of view. The studies of counterfactual phenomena of quantum mechanics are presented, where quantum the Cheshire-Cat is generated and observed using a neutron interferometer set-up: neutron and its spin are disembodied. Note that weak values, which are defined and obtained by pre- and postselection together with special estimation strategy of the intermediate state, allow to create and confirm the quantum Cheshire-Cat.

1. Arndt, M., Ekers, A., von Klitzing, W. and Ulbricht, H., Focus on modern frontiers of matter wave optics and interferometry. *New J. Phys*., 2012, **14**, 125006-1 to 125006-9, and references therein.
2. Feynman, R. P., Leighton, P. B. and Sands, M. L., *The Feynman Lectures on Physics, Vol. III: Quantum Mechanics*, Addision-Wesley, 1965.
3. Popescu, S., Dynamical quantum non-locality. *Nature Phys*., 2010, **6**(2), 151–153.
4. Rauch, H., Treimer, W. and Bonse, U., Test of a single crystal neutron interferometer. *Phys. Lett. A*, 1974, **47**(5), 369–371.
5. Rauch, H. and Werner, S. A., *Neutron Interferometry*, Oxford University Press, 2015.
6. Hasegawa, Y. and Rauch, H., Quantum phenomena explored with neutrons. *New J. Phys*., 2011, **13**, 115010-1 to 115010-18.
7. Mezei, F., *Neutron Spin Echo, Lecture Notes in Physics*, Springer, 1980, vol. 128.
8. Klepp, J., Sponar, S. and Hasegawa, Y., Fundamental phenomena of quantum mechanics explored with neutron interferometers. *Prog. Theor. Exp. Phys*., 2014, **2014**(8), 082A01-1 to 082A01-61.
9. Hasegawa, Y. and Badurek, G., Noncommuting spinor rotation due to balanced geometrical and dynamical phases. *Phys. Rev. A,* 1999, **59**(6), 4614–4622.
10. Klepp, J., Sponar, S., Filipp, S., Lettner, M., Badurek, G. and Hasegawa, Y., Observation of nonadditive mixed-state phases with polarized neutrons. *Phys. Rev. Lett.*, 2008, **101**(15), 150404-1 to 150404-4.
11. Erhart, J., Sponar, S., Sulyok, G., Badurek, G., Ozawa, M. and Hasegawa, Y., Experimental demonstration of a universally valid error–disturbance uncertainty relation in spin measurements. *Nature Phys*., 2012, **8**(3), 185–189.
12. Sulyok, G., Sponar, S., Erhart, J., Badurek, G., Ozawa, M. and Hasegawa. Y., Violation of Heisenberg's error–disturbance uncertainty relation in neutron-spin measurements. *Phys. Rev. A*, 2013, **88**(2), 022110-1 to 022110-15.
13. Ozawa, M., Universally valid reformulation of the Heisenberg uncertainty principle on noise and disturbance in measurement. *Phys. Rev. A*, 2003, **67**, 042105; Ozawa, M., Physical content of Heisenberg's uncertainty relation: limitation and reformulation. *Phys. Lett. A*, 2003, **318**(1-2), 21–29.
14. Ozawa, M., Uncertainty relations for noise and disturbance in generalized quantum measurements. *Ann. Phys.* (*N.Y.*), 2004, **311**(2), 350–416.
15. Aharonov, Y. and Rohrlich, D., *Quantum Paradoxes: Quantum Theory for the Perplexed*, Wiley-VCH, 2005.
16. Aharonov, Y., Popescu, S., Rohrlich, D. and Skrzypczyk, P., Quantum Cheshire Cats. *New J. Phys*., 2013, **15**, 113018-1 to 113018-9.
17. Denkmayr, T., Geppert, H., Sponar, S., Lemmel, H., Matzkin, A., Tollaksen, J. and Hasegawa, Y., Observation of a quantum Cheshire Cat in a matter-wave interferometer experiment. *Nature Commun*., 2014, **5**, 4492-1 to 4492-7.
18. Wheeler, J. A. and Zurek, W. H. (eds), *Quantum Theory and Measurement*, Princeton University Press, 1983.
19. Heisenberg, W., Über den anschaulichen inhalt der quantentheoretischen kinematik und mechanic – The actual content of quantum theoretical kinematics and mechanics. *Z. Phys.*, 1927, **43**(3–4), 172–198.
20. Kennard, E. H., Zur quantenmechanik einfacher bewegungtypen. *Z. Phys.*, 1927, **44**(4–5), 326–352.
21. Robertson, H. P., The uncertainty principle. *Phys. Rev*., 1929, **34**(1), 163–164; Schrödinger, E., Zum Heisenbergschen unschärfeprinzip. *Sitzungsberichte Preus. Akad. Wiss., Phys.-Math. Klasse*, 1930, **14**, 296–303.
22. Rozema, L. A., Darabi, A., Mahler, D. H., Hayat, A., Soudagar, Y. and Steinberg, A. M., Violation of Heisenberg's measurement–disturbance relationship by weak measurements. *Phys. Rev. Lett.*, 2012, **109**(10), 100404-1 to 100404-5.
23. Baek, S.-Y., Kaneda, F., Ozawa, M. and Edamatsu, K., Experimental violation and reformulation of the Heisenberg's error–disturbance uncertainty relation. *Sci. Rep.*, 2013, **3**, 2221-1 to 2221-5.
24. Weston, M. M., Hall, M. J. W., Palsson, M. S., Wiseman, H. M. and Pryde, G. J., Experimental test of universal complementarity relations. *Phys. Rev. Lett.*, 2013, **110**(22), 220402-1 to 220402-5.
25. Branciard, C., Error–tradeoff and error–disturbance relations for incompatible quantum measurements. *Proc. Natl. Acad. Sci. USA*, 2013, **110**(17), 6742–6747.
26. Ringbauer, M., Biggerstaff, D. N., Broome, M. A., Fedrizzi, A., Branciard, C. and White, A. G., Experimental joint quantum measurements with minimum uncertainty. *Phys. Rev. Lett.*, 2014, **112**(2), 020401-1 to 020401-5.
27. Kaneda, F., Baek, S.-Y., Ozawa, M. and Edamatsu, K., Experimental test of error–disturbance uncertainty relations by weak measurement. *Phys. Rev. Lett.*, 2014, **112**(2), 020402-1 to 020402-5.
28. Lu, X.-M., Yu, S., Fujikawa, K. and Oh, C. H., Improved error–tradeoff and error–disturbance relations in terms of measurement error components. *Phys. Rev. A*, 2014, **90**(4), 042113-1 to 7, and references therein.
29. Busch, P., Lahti, P. and Werner, R. F., Proof of Heisenberg's error–disturbance relation. *Phys. Rev. Lett.*, 2013, **111**(16), 160405-1 to 160405-5.
30. Rozema, L. A., Mahler, D. H., Hayat, A. and Steinberg, A. M., A note on different definitions of momentum disturbance. *Quantum Stud.: Math. Found*., 2013, **2**(1), 17–22.
31. Ozawa, M., Disproving Heisenberg's error–disturbance relation. arXiv:1308.3540[quant-ph].
32. Korzekwa, K., Jennings, D. and Rudolph, T., Operational constraints on state-dependent formulations of quantum error–disturbance trade-off relations. *Phys. Rev. A*, 2014, **89**(5), 052108-1 to 052108-6.
33. Buscemi, F., Hall, M. J. W., Ozawa, M. and Wilde, M. M., Noise and disturbance in quantum measurements: an information theoretic approach. *Phys. Rev. Lett.*, 2014, **112**(5), 050401-1 to 050401-5.
34. Sulyok, G., Sponar, S., Demirel, B., Busemi, F., Hall, M. J., Ozawa, M. and Hasegawa, Y., Experimental test of entropic noise-disturbance uncertainty relations for spin-1/2 measurements. *Phys. Rev. Lett.*, 2015, **115**(3), 030401-1 to 030401-5.
35. Schrödinger, E., Die gegenwartige situation in der quantenmechanik. *Naturwissenschaften*, 1935, **23**(48), 807–812.
36. Einstein, A., Podolsky, B. and Rosen, N., Can quantum-mechanical description of physical reality be considered complete? *Phys. Rev*., 1935, **47**(10), 777–780.
37. Hardy, L., Quantum mechanics, local realistic theories, and Lorentz-invariant realistic theories. *Phys. Rev. Lett.*, 1992, **68**(20), 2981–2984.

38. Lundeen, J. S. and Steinberg, A. M., Experimental joint weak measurement on a photon pair as a probe of Hardy's paradox. *Phys. Rev. Lett.*, 2009, **102**(2), 020404-1 to 020404-4.
39. Yokota, K., Yamamoto, T., Koashi, M. and Imoto, N., Direct observation of Hardy's paradox by joint weak measurement with an entangled photon pair. *New J. Phys.*, 2009, **11**, 033011-1 to 033011-9.
40. Aharonov, Y., Albert, D. Z. and Vaidman, L. H., How the result of a measurement of a component of the spin of a spin-1/2 particle can turn out to be 100. *Phys. Rev. Lett.*, 1988, **60**(14), 1351–1354.
41. Duck, I. M., Stevenson, P. M. and Sudarshan, E. C. G., The sense in which a 'weak measurement' of a spin-1/2 particle's spin component yields a value 100. *Phys. Rev. D*, 1989, **40**(6), 2112–2117.
42. Ritchie, N. W. M., Story, J. G. and Hulet, R. G., Realization of a measurement of a 'weak value'. *Phys. Rev. Lett.*, 1991, **66**(9), 1107–1110.
43. Jozsa, R., Complex weak values in quantum measurement. *Phys. Rev. A*, 2007, **76**(4), 044103-1 to 044103-3.
44. Hosten, O. and Kwiat, P., Observation of the spin Hall effect of light via weak measurements. *Science*, 2008, **319**(5864), 787–790.
45. Hasegawa, Y., Investigations of fundamental phenomena in quantum mechanics with neutrons. *J. Phys. Conf. Ser.*, 2014, **504**, 012025-1 to 012025-13.

ACKNOWLEDGEMENTS. We thank all our colleagues who were involved in carrying out the experiments presented here; in particular, G. Badurek, B. Demirel, T. Denkmayr, J. Erhart, H. Geppert, A. Hosoya, H. Lemmel, A. Matzkin, M. Ozawa, H. Rauch, S. Sponar, G. Sulyok and J. Tollaksen. This work was partially supported by the Austrian FWF (Fonds zur Föderung der Wissenschaftlichen Forschung) through grant numbers P25795-N20 and P27666-N20. Some parts of the results presented here have appeared in an earlier conference review article[45].

doi: 10.18520/v109/i11/1972-1979